Journal of Achievements in Materials and Manufacturing Engineering
VOLUME 61
ISSUE 2
December
2013

Properties of $Fe_{73}Ni_5Y_3B_{19}$ amorphous ribbon produced by melt-spinning

K. Zdrodowska [a,*], P. Kwarciak [a], M. Szota [a], M. Nabiałek [b]
[a] Institute of Materials Engineering, Faculty of Production Engineering and Materials Technology, Czestochowa University of Technology,
[b] Institute of Physics, Faculty of Production Engineering and Materials Technology, Czestochowa University of Technology
* Corresponding e-mail address: kzdrodowska@wip.pcz.pl

Received 21.10.2013; published in revised form 01.12.2013

Manufacturing and processing

ABSTRACT

Purpose: The purpose of the study is to examine the mechanical properties of $Fe_{73}Ni_5Y_3B_{19}$, alloy and to carry out the comparative examination of matt and glossy sides of those alloys.
Design/methodology/approach: The $Fe_{73}Ni_5Y_3B_{19}$, alloy have been produced by the melt-spinning method which involves rapid cooling of the metal on a spinning copper cylinder. The cooling rate has required for obtaining the amorphous alloy ranges from 10 5 to 106 K/s. The above-mentioned method is popular and often used; however, in order to obtain alloys of amorphous structure, it should be assured that the conditions for obtaining amorphous materials, as set by A. Inoe, are satisfied.
Findings: Mechanical properties, such as microhardness, roughness, abrasive wear with the use of a ball tester, have been described and the X-ray diffraction has been determined in the paper.
Research limitations/implications: Analyzed modernization of the machine refers to pin on disc, disc-disc, block and disc unit sliding friction processes.
Practical implications: The $Fe_{73}Ni_5Y_3B_{19}$ amorphous alloys find the application in the power industry, where they are used for transformer cores.
Keywords: Amorphous alloys; Melt-spinning; Ribbon

Reference to this paper should be given in the following way:
K. Zdrodowska, P. Kwarciak, M. Szota, M. Nabiałek, Properties of $Fe_{73}Ni_5Y_3B_{19}$ amorphous ribbon produced by melt-spinning, Journal of Achievements in Materials and Manufacturing Engineering 61/2 (2013) 381-388.

1. Introduction

Many renowned scientists addressed the issue of amorphous alloys as materials being in forward-looking group of engineering materials. One of the most famous people dealing with issues of metallic glasses is A. Inoue. It was him who formulated the rules for the production of amorphous alloys [1-2].

An important parameter defining the ability of the alloy to pass into an amorphous state is, the reduced temperature of the glass transition and is defined as:

$$\frac{TG}{Tm} \quad (1)$$

where:
T_G - the temperature of the glass transition
T_m - melting point

In order to increase the ability of the alloy to pass in an amorphous state, it should be strived in order to increase the temperature of T_G, while decreasing the value of the parameter

© Copyright by International OCSCO World Press. All rights reserved. 2013

T_m. The purpose of such an action is to reduce the temperature of glass transition into 1. The increase in the value of T_G/T_m will reduce the amount of heat which must be collected from the alloy in the liquid state, so that the temperature was in the glass transition. Another parameter introduced by A. Inoue is the size of the supercooled area, which is denoted as ΔTx, the value is proportional to the ability to pass the melt into an amorphous state. The cooling below the crystallization temperature of the alloy is possible when the cooling rate is reduced if there is an increase of the supercooling region, while the glass transition point is remote from the melt crystallization point. Another parameter determining the ability of the melt to the glass transition is a critical cooling rate R_C. Reducing the critical cooling rate causes the increase in capacity of the alloy at the glass transition temperature. This parameter also affects the thickness of the obtained material. The value of the critical cooling rate for Fe-based alloys is at the range of 10^6 K/s [1-4].

Achieving the amorphous structure of the alloy is possible if the temperature is cooled from above Tm, at a rate equal to or greater than the R_C to a temperature T_G. The type of cooling system is that it does not occur in the melt to crystallize during cooling from the liquid phase and the amorphous structure is formed. The melt crystallization process occurs when the cooling rate is less than the critical cooling rate, and the resulting material does not have the amorphous structure as well as the desired properties. Amorphous ribbon are prepared by a rapid cooling on a rotating copper roll rotating at a cooling rate of 10^5 for 10^6 K/s, the method is called melt - spinning. Alloys consist of more than three components, the first of which should be a transition metal or its combination, another metalloid or its combination. The selected components should have the ability to form the amorphous state. If the main components have negative heat of mixing, the energy gap at the interface when connects material increases. The viscosity of the melt increases, and it causes a reduction of migration of atoms leading to the formation of crystalline phase nucleation [1-5].

Alloys having in their composition transition metals such as cobalt, iron or nickel easily undergo through the glass transition processes. The process is also needed for the addition of metalloid, which allows for lowering a critical cooling rate. Those metalloids include carbon, boron or silicon. The glass transition of the amorphous alloy is obtained by cooling faster than the critical speed. The cooling stops at a predetermined speed and it can be partially crystallized structure. It is a reversible process and the metallic glass by heating from room temperature starts to crystallize. Also, long-term holding at an elevated temperature will lead to the formation of crystalline structures [6-8].

The use of amorphous alloys is very broad, because they are used in production of i.e. golf clubs, cell phone housing, surgical instruments, or the cores of transformers. Their examples are presented in Fig. 1. The use of amorphous glass is closely related to their chemical composition, as well as methods and conditions of preparation [9-13].

In Poland, the study of amorphous ribbons was initiated by the Institute of the Polish Academy of Sciences, Institute of Materials Science and Engineering, Warsaw University of Technology, Institute of Non-Ferrous Metals in Gliwice as well as the Institute of Physics and Institute of Materials Science and Engineering University of Czestochowa [1,2].

Fig. 1. The use of amorphous alloys for golf clubs, implants, phone housing [9-11]

There are also many other possibilities of the application of thin-layered amorphous ribbons, primarily in electrical equipment. They are used for electric measuring systems and supervisory control systems, conductors, magnetic sensors, pressure pick-ups. It provides a possibility of their practical use in many branches of industry, e.g. the automotive, electrical and aircraft industries, as well as in medicine. The magnetic properties of the metallic glass ribbons depend on the composition, production procedure and the condition of heat treatment [14-16].

The purpose of the work was to make thin-film Fe73Ni5Y3B19 amorphous ribbons, and to study their mechanical properties.

In order to characterise achieved ribbons the following tests: metallographic, microhardness, resistance tribological ones using a bulletproof tester and surface roughness profile, and a X-ray one have been carried out.

2. Testing material and research methodology and analysis of the testing results

The paper presents the results of thin-film $Fe_{73}Ni_5Y_3B_{19}$ alloys produced by melt - spinning. Boron was added as a melt of known chemical composition FeB. Initial remelting of the components was done using an electric arc in the presence of an inert gas. The ingots were cleaned and segregated into charge batches and placed in an induction furnace, where then the ribbon production process took place. For production of ribbons, a method involving the continuous casting of the liquid alloy on a spinning copper drum, a so-called melt-spinning method, was

employed. The investigations were carried out for the $Fe_{73}Ni_5Y_3B_{19}$ alloy. In order to assess the mechanical properties, metallographic examinations, microhardness tests, tribological resistance tests using a ball tester, surface roughness profile examinations, as well as an X-ray analysis, were carried out. Table 1 presents the composition of the sample.

Table.1.
The chemical composition of the $Fe_{73}Ni_5Y_3B_{19}$ tested sample

Sample number	Chemical composition
1	$Fe_{73}Ti_5Y_3B_{19}$

Fig. 2. The research material in $Fe_{73}Ni_5Y_3B_{19}$ ribbon

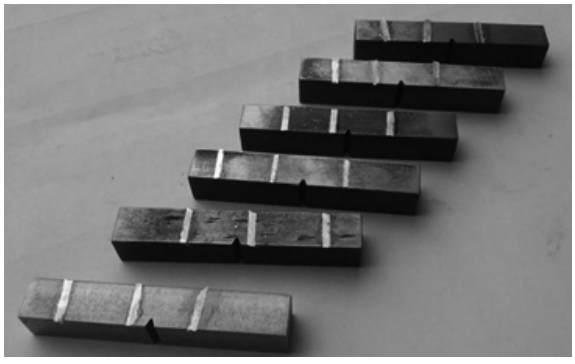

Fig. 3. Ribbons amorphous samples prepared for testing

Ribbons with metallic glasses used in the study were prepared at the Technical University of Czestochowa. Figure 2 shows the $Fe_{73}Ni_5Y_3B_{19}$ ribbon amorphous

In order to carry out the planned investigations, the amorphous ribbons has to be suitably prepared. Ribbon lengths for comparing mechanical properties were stuck on identical impact test specimens. In the paper an attention is drawn to the fact that each ribbon has a bright and a matt side. The matt side is formed at the cylinder side, while the bright side is an outer one. The specimens prepared for testing are shown in Fig. 2.

2.1. X-ray analysis

An X-ray analysis was made using an X-ray diffractometer, which was equipped with a cobalt tube with the CuK_α characteristic radiation. The sample was irradiated with X-rays in the angle range from 30° to 120°, with a measurement step of 0.2° and an exposure time of 3s. Figure 4 shows the $Fe_{73}Ni_5Y_3B_{19}$ X-ray diffraction.

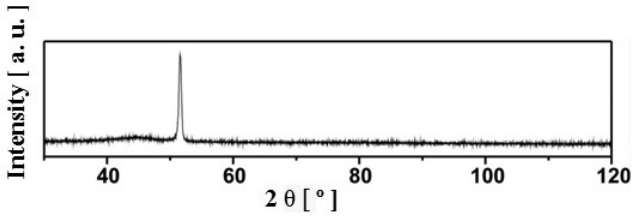

Fig. 4. An X-ray diffraction for $Fe_{73}Ni_5Y_3B_{19}$

In Figure 4 X-ray diffraction pattern for the $Fe_{73}Ni_5Y_3B_{19}$ alloy is presented. Amorphous materials do not have ordered crystalline structure. X-ray diffraction shows an amorphous phase, but not in the entire volume. The formation of the crystalline phase is crucial for the chemical composition and the percentage of the individual components.

2.2. Microhardness

Microhardness tests were performed by the Vickers method using a Future-Tech FM7 microhardness tester. The load was 490.3 mN, while the loading time 6 seconds. Five indentations were made for each ribbon. The tests results are summarized in Table 2.

Table.2.
Microhardness measurement results for HV0.05 for $Fe_{73}Ni_5Y_3B_{19}$

Number of measurement	Matt side	Glossy side
1	920.7	1091.9
2	1060.6	1095.5
3	941.3	1088.4
4	991.6	1146.0
5	648.2	1076.7
Średnia Wartość	912.48	1099.7

The growth of micro-hardness measurements for the glossy side is visible but the difference in results between glossy and matte sides is small enough that it can be concluded that within the limits of error.

2.3. Tribological tests using the ball tester

The next stage of the investigations included abrasion testing. Each of the alloys was subjected to a one-, two- and three-hours' test during ball testing. A 20 mm-diameter zirconium ball was used. Then, obtained abrasions were figure at a magnification 50x (Figs. 5-6).

2.4. Surface roughness profiles

For the determination of the surface roughness of the specimens, an Hommel T1000 profilometer was used. The examination was made along a measuring length of 1.5 mm. Figures 7-12 present selected graphs illustrating the surface roughness profiles of the $Fe_{73}Ni_5Y_3B_{19}$ ribbon on the matt and the glossy side, respectively. Tables 3-4 summarizes selected roughness parameter results. The images of the roughness profiles after approximation and the information on the magnitudes of the roughness parameters were obtained using the software supplied with the Hommel T1000 profilometer.

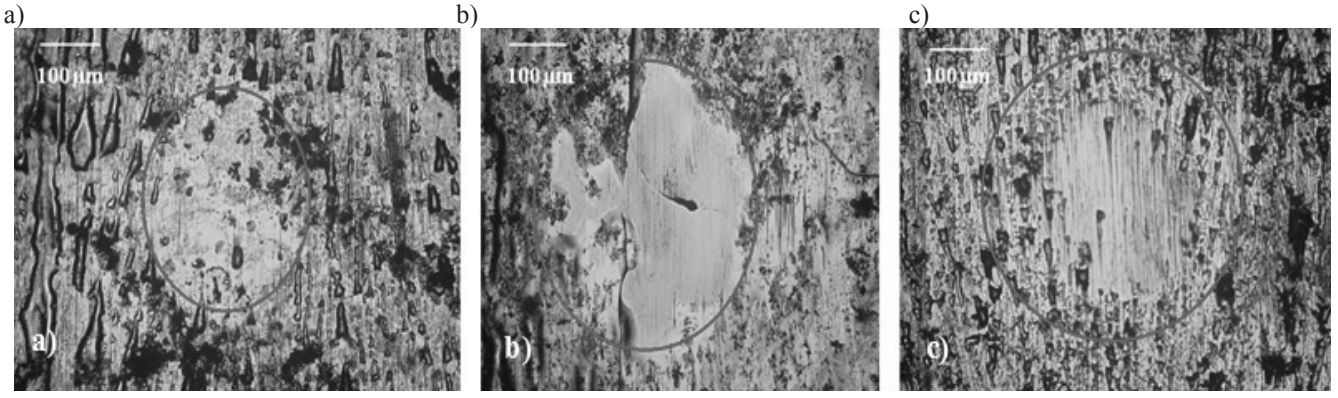

Fig. 5. Abrasions on the glossy side of the $Fe_{73}Ni_5Y_3B_{19}$ ribbon after, respectively, 1 hr,2 hrs and 3 hrs

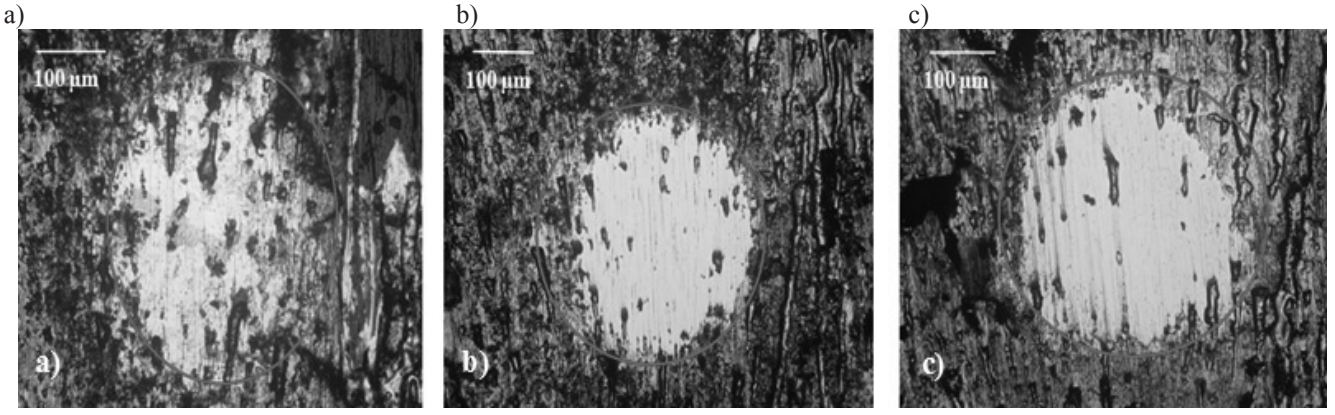

Fig. 6. Abrasions on the matt side of the $Fe_{73}Ni_5Y_3B_{19}$ ribbon after, respectively, 1 hr,2 hrs and 3 hrs

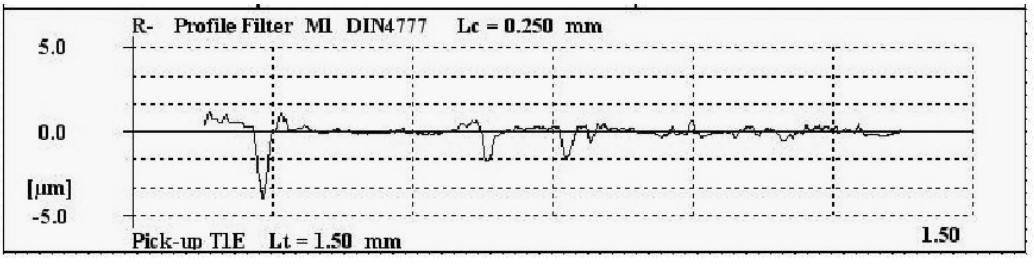

Fig. 7. The roughness profile of the $Fe_{73}Ni_5Y_3B_{19}$ ribbon at the matt side after an abrasion time of 1 hr.

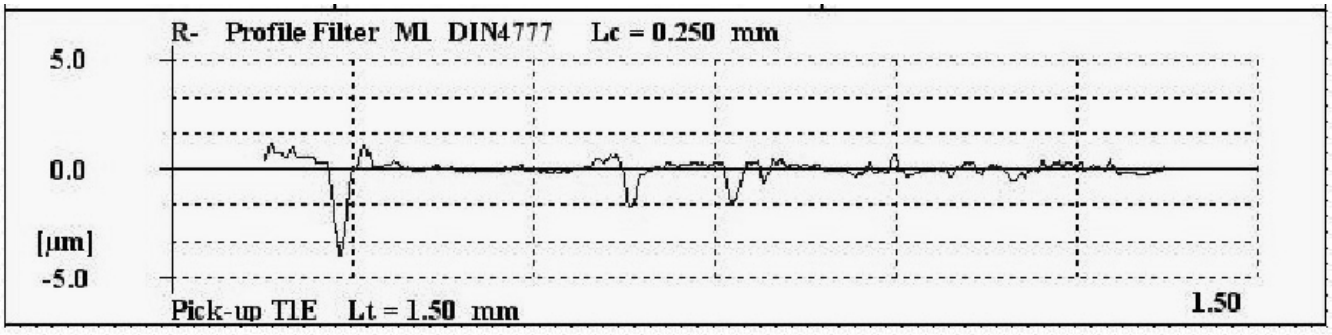

Fig. 8. The roughness profile of the $Fe_{73}Ni_5Y_3B_{19}$ ribbon at the matt side after an abrasion time of 2 hr

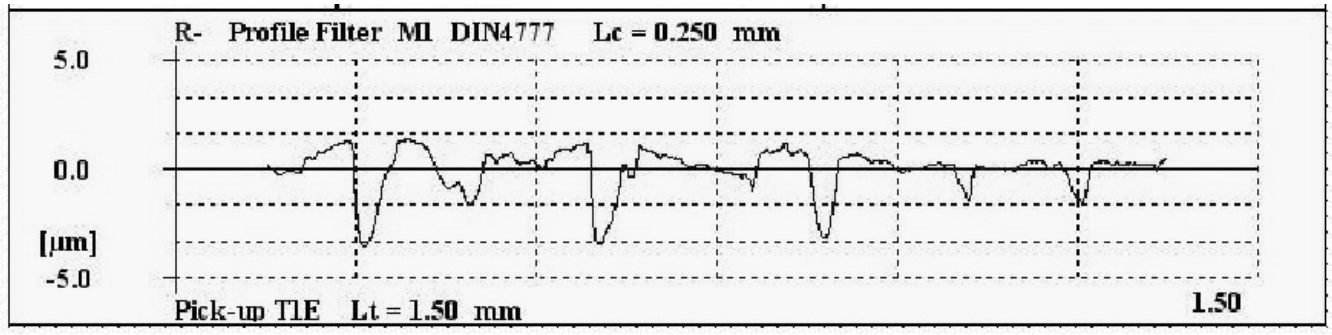

Fig. 9. The roughness profile of the $Fe_{73}Ni_5Y_3B_{19}$ ribbon at the matt side after an abrasion time of 3 hr

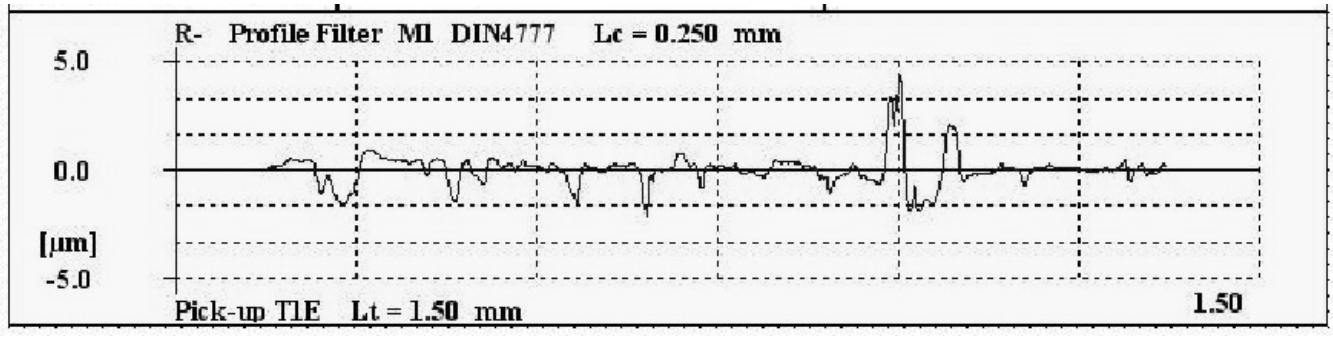

Fig. 10. The roughness profile of the $Fe_{73}Ni_5Y_3B_{19}$ ribbon at the glossy side after an abrasion time of 1 hr

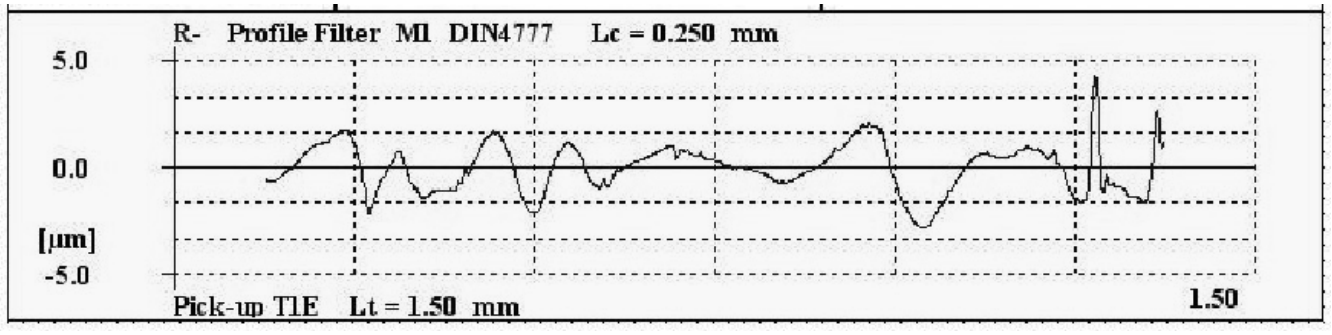

Fig. 11. The roughness profile of the $Fe_{73}Ni_5Y_3B_{19}$ ribbon at the glossy side after an abrasion time of 2 hr

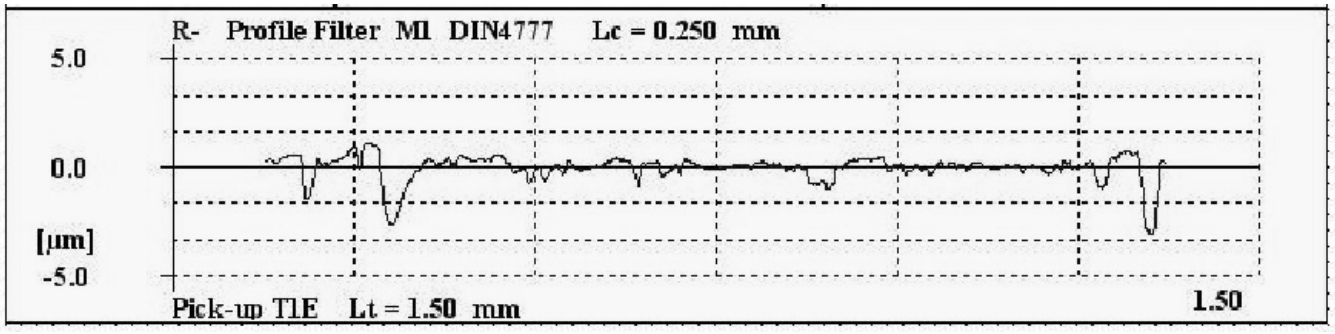

Fig. 12. The roughness profile of the $Fe_{73}Ni_5Y_3B_{19}$ ribbon at the glossy side after an abrasion time of 3 hr

Table.3.
Measurement results of roughness parameters for the $Fe_{73}Ni_5Y_3B_{19}$ alloy at the glossy side

Material	Roughness parameters		
	R_a [µm]	R_{max} [µm]	R_z [um]
$Fe_{73}Ni_5Y_3B_{19}$	0.95	6.35	3.04

Table.4.
Measurement results of roughness parameters for the $Fe_{73}Ni_5Y_3B_{19}$ alloy at the matt side

Material	Roughness parameters		
	R_a [µm]	R_{max} [µm]	R_z [µm]
$Fe_{73}Ni_5Y_3B_{19}$	2.20	5.18	0.29

The surface roughness profile examinations showed a difference for both the matt and the glossy sides of the $Fe_{73}Ni_5Y_3B_{19}$ ribbon alloy. Differences show such parameters as R_a and R_z. This is due to the cooling conditions and adjustment of the chemical composition.

3. Conclusions

The results of micro-hardness measurements for HV0. 05 alloy $Fe_{73}Ni_5Y_3B_{19}$ show an increase in the hardness of the glossy side. The result is repeated for all five measurements. Thin-layer ribbon was significantly different both at the matte and glossy side. The profilometer showed differences in the roughness of the strip, depending on the test side. The matte surface roughness parameters such as Ra, Rz and Rmax equal to 2.20 µm, 0.29 µm and 5.18 µm , while the shiny side is 0.95 µm, 3.04 µm and 6.35 µm. The crystalline phase formation was shown in X-ray diffractometer but not in the entire volume.

References

[1] K. Zdrodowska, P. Kwarciak, J. Jędryka, M. Szota, M. Nabiałek, Materials Engineering 4 (2013) 401-404.
[2] A. Baron, D. Szweiczek, G. Nawrat, Corrosion of amorphous and nanocrystalline Fe-based alloys and its influence on their magnetic behavior, Electrochimica Acta 52 (2007) 5690-5695.
[3] Żak, W. Burian, A rig for casting massive amorphous alloys, IMŻ 4 (2010) 35-40.
[4] J. Zbroszczyk, Amorphous and nanocrystalline iron alloys Publishing House University of Czestochowa, vol. 134 Czestochowa, 2007.
[5] Inoue, Bulk amorphous alloys, Preparation and fundamental characteristic, Materials Science Foundation's 6 (1998).
[6] Inoue, Bulk amorphaus alloys with soft and hard magnetic properties, Materials Science and Engineering A 226-228 (1997) 357-363.
[7] D. Szewiczek, J. Tyrlik-Held, S. Lesz, Changes of mechanical properties and fracture morphology of amorphous tapes involved by heat treatment, Journal of Materials Processing Technology 109 (2001) 190-195.
[8] D. Pavuna, Production of metallic glass ribbons by the chill-block meltspinning technique in stabilized laboratory conditions. Journal of Materials Science 16 (9) (1981) 2419-2433.
[9] http://www.strefamobile.pl/aktualnosci/1977/iphone-6-z-obudowa-liquidmetal.
[10] http://luxluxlux.pl/2011/09/18/magia-golfa-czyli-gra-wszechczasow/.
[11] http://www.stomatologiagrzesiak.pl/oferta/implanty.
[12] H.S. Lesz, R. Babilas, M. Nabiałek, Szota, M. Dośpiał, R. Nowosielski, The characterization of structure, thermal

stability and magnetic properties of Fe-Co-B-Si-Nb bulk amorphous and nanocrystalline alloys, Amorphous and Nanostructured Materials (2011) 197-201.

[13] M. Nabiałek, M. Dośpiał, M. Szota, P. Pietrusiewicz, S. Walters, D. Skowron, Investigation of magnetic properties of $Fe_{61}Co_8Zr_{4-x}Y_{2+x}Ni_5Nb_5B_{15}$amorphous alloys (x = 0, 1) in the form of ribbons. Materials Science and Engineering B 2012 MSB-13231.

[14] S. Lesz, R. Babilas, M. Nabiałek, M. Szota, M. Dośpiał, R. Nowosielski, The characterization of structure, thermal stability and magnetic properties of Fe-Co-B-Si-Nb bulk amorphous and nanocrystalline alloys, Journal of Alloys and Compounds 509S (2011) 197-S201

[15] R. Nowosielski, J.J. Wysłocki, I. Wnuk, R. Gramatyka,: Nanocrystalline soft magnetic composite cores, Journal of Materials Processing Technology 175 (2006) 324-329.

[16] S.W. Du, R.V. Ramanujan, Crystallization and magnetic properties of Fe40Ni38B18Mo4 amorphous alloy, Journal of Non-Crystalline Solids 351 (2005) 3105-3113.